Eur. Phys. J. B **3**, 263–270 (1998)

THE EUROPEAN PHYSICAL JOURNAL B

Transmission resonances in magnetic-barrier structures

Y. Guo[1,2,a], Z.-Q. Li[2], B.-L. Gu[1], Q. Sun[2], J.-Z. Yu[2], and Y. Kawazoe[2]

[1] Department of Physics, Tsinghua University, Beijing 100084, P.R. China
[2] Institute for Materials Research, Tohoku University, Sendai 980-8577, Japan

Received: 18 August 1997 / Revised: 20 September 1997 / Accepted: 13 October 1997

Abstract. Quantum transport properties of electrons in simple magnetic-barrier (MB) structures and in finite MB superlattices are investigated in detail. It is shown that there exists a transition of transmission resonances, *i.e.*, from incomplete transmission resonances in simple MB structures consisting of unidentical blocks, to complete transmission resonances in comparatively complex MB structures ($n \geq 4$, n is the number of barriers). In simple unidentical block arrangements in double- and triple-MB structures we can also obtain complete transmission by properly adjusting parameters of the building blocks according to k_y-value (k_y is the wave vector in y direction). Strong suppression of the transmission and of the conductance is found in MB superlattices which are periodic arrangements of two different blocks. The resonance splitting effect in finite MB superlattices is examined. It is confirmed that the rule (*i.e.*, for n-barrier tunneling the splitting would be $(n-1)$-fold) obtained in periodic electric superlattices can be extended to periodically arranged MB superlattices of identical blocks through which electrons with $k_y \geq 0$ tunnel, and it is no longer proper for electrons with $k_y < 0$ to tunnel.

PACS. 73.40.Gk Tunneling – 03.65.Ge Solutions of wave equations: bound states

1 Introduction

Since the proposal and realization of the semiconductor heterojunction superlattice (SL) by Esaki and Tsu [1] and by Chang *et al.* [2] in the early 70s, electron transport phenomena in the superlattice have attracted tremendous interest and become a frontier research field. Over past years, the electronic properties of the SL have been the subject of active studies, both theoretically and experimentally, due to the demand to understand the physics involved and its great technological potential. One important feature revealed by studies on comparatively simple structures such as double-barrier structures (DBS) and triple-barrier structures (TBS), is the resonant tunneling. The resonance splitting effect was found from the studies on multiple-barrier tunneling. A resonance peak of the transmission coefficient in a DBS splits into a doublet while in a TBS and quadruplets in a quintuple-barrier structures [3]. The feature was extended directly to a general case: for n-barrier tunneling the splitting would be $(n-1)$-fold. Furthermore, Tsu and Esaki [3] pointed out that the split resonance energies would eventually approach to the band model results for very large n. The above generalization was proved analytically by Liu and Stamp [4] at zero bias.

Recently there has been increased interest in studying the behavior of two-dimensional electron gas (2DEG) subjected to inhomogeneous magnetic field on a nanometer scale. Experimentally this kind of field has been realized with creation of magnetic dots [5], patterning of ferromagnetic materials [6], and deposition of superconducting materials on conventional heterostructures [7]. Transport of electrons in a unidirectional weak magnetic field modulation has been realized by Carmona *et al.* [8], Ye *et al.* [9] and Izawa *et al.* [10]. They observed oscillatory magnetoresistance due to a commensurability effect between the classical cyclotron diameter and the period of magnetic modulation. These experimental techniques open up the way to experiments in alternating magnetic fields with periods in the nanometer region. Theoretically, the tunneling properties through a thick potential barrier under the influence of a local magnetic field was investigated by Ramaglia *et al.* [11] who found that the magnetic field was localized strictly within the potential barrier, which led to resonances that were centered within the barrier. The motion of 2DEG in an finite strip across which a magnetic field varies linearly [12], in a smooth magnetic barrier geometry of different shape [13] and in a curved 2DEG system were also studied [14]. Very recently, studies on electron tunneling through symmetric magnetic barriers [15,16] and asymmetric magnetic barriers [17] showed that magnetic barriers possess wave-vector filtering properties and the asymmetric double-barrier magnetic structure possess stronger filtering properties. Quantum transport through periodically arranged magnetic barriers [18] and magnetic superlattices [19] has also been dealt with.

[a] e-mail: guoy@phys.tsinghua.edu.cn

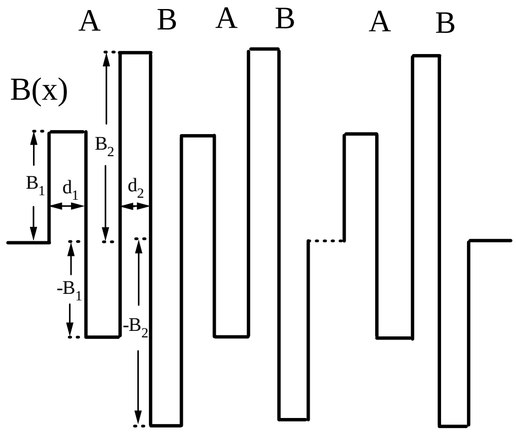

Fig. 1. Magnetic superlattice made up of two different building blocks A and B.

The latter study found the energy spectrum consists of magnetic minibands.

In this paper we will be concerned with electronic transport properties in simple MB structures (such as double MB structure (DMBS) and triple MB structure (TMBS)), in comparatively complex MB structures (such as quadruple MB structure(QMBS) *etc.*), and in finite MB superlattices which are modeled by periodically arranged magnetic barriers and magnetic wells. We find that there exists a transition of transmission resonances for electrons transport from simple MB structures of unidentical blocks to comparatively complex MB structures arranged by two different blocks, complete transmission resonances can be seen in the latter case as in MB structures of identical blocks. We also explore the possibility of complete tunneling in simple MB structures arranged by different blocks. The resonance splitting effect in finite MB superlattices is investigated, similarities and differences of splitting features between MB superlattices and electrostatic superlattices are discussed. Our studies show that resonance splitting phenomena is more complex in the MB superlattice, and its features depend strongly not only on the geometry of building blocks but also on orientations of the wave vector of incident electrons.

2 Theory

Now we consider a 2DEG system (in (x, y) plane) subject to a perpendicular magnetic field (along z direction) as depicted in Figure 1. The magnetic field is taken to be homogeneous along y axis and varies along x axis. The total magnetic field over the whole 2DEG plane is zero. A MB superlattice can be obtained by periodically arranging two different blocks A and B. Each building block consists of one magnetic barrier (with height B_i and width d_i $(i = 1, 2)$) and one magnetic well (with height $-B_i$ and width d_i $(i = 1, 2)$). We take rectangular profile of $B(x)$ which is the limit of small distance between 2DEG and ferromagnetic thin film. The Schrödinger equation is written in the framework of the effective mass approximation in each magnetic barrier and well region as

$$\frac{1}{2m^*}[\mathbf{P} + e\mathbf{A}_i]^2\psi(x, y) = E\psi(x, y), \tag{1}$$

where m^* is the electron effective mass, and $\mathbf{A}_i$ the Landau vector potential which is taken in the Landau gauge $\mathbf{A}_i = (0, A_i(x), 0)$, in which

$$A_i(x) = \begin{cases} B_1[x - (m-1)(d_1 + d_2)], \\ (m-1)(d_1 + d_2) \le x < md_1 + (m-1)d_2, \\ -B_1[x - (m+1)d_1 - (m-1)d_2], \\ md_1 + (m-1)d_2 \le x < (m+1)d_1 + (m-1)d_2, \end{cases}$$
$$m = 1, 3, 5, \cdots, \tag{2a}$$

$$A_i(x) = \begin{cases} B_2[x - md_1 - (m-2)d_2], \\ md_1 + (m-2)d_2 \le x < md_1 + (m-1)d_2, \\ -B_2[x - m(d_1 + d_2)], \\ md_1 + (m-1)d_2 \le x < m(d_1 + d_2), \end{cases}$$
$$m = 2, 4, \cdots, \tag{2b}$$

where m is the order number of magnetic barriers or wells.

For convenience, we express all quantities in dimensionless units by using the cyclotron frequency $\omega_c = eB_0/m^*$ and the magnetic length $l_B = \sqrt{\hbar/eB_0}$. For GaAs and an estimated $B_0 = 0.1$ T we have $l_B = 813$ Å, $\hbar\omega_c = 0.17$ meV [15]; m^* can be taken as $0.067m_e$ (m_e is the free electron mass). The coordinate $\mathbf{r}$ is in unit of l_B, A_i in unit of $B_0 l_B$, the energy E in unit of $\hbar\omega_c$. Since the y component of electron momentum operator commutes with the Hamiltonian, the wave function can be written as a product $\psi(x, y) = e^{ik_y y}\psi(x)$, where k_y is the wave vector of the electron in the y direction. Accordingly, we obtain the following 1D Schrödinger equation

$$\left\{\frac{d^2}{dx^2} - [A_i(x) + k_y]^2 + 2E\right\}\psi(x) = 0. \tag{3}$$

The function $V(x, k_y) = [A_i(x) + k_y]^2/2$ can be interpreted as a k_y-dependent electric potential. Notice that the effective potential for electron motion in the x direction depends on the electron wave vector in the y direction. In the left and the right regions, the wave functions are free electron wave functions, which can be written as $\psi_l(x) = e^{ik_l x} + re^{-ik_l x}$, and $\Psi_r(x) = \tau e^{ik_r x}$, where $k_i = \sqrt{2E - [A_i(x) + k_y]^2} (i = l, r)$.

In magnetic barrier and well regions, the wave function $\psi_i(x)$ can be written as a linear combination of Hermitian functions [20]

$$\Psi_i(x) = \exp(-\frac{\xi_i^2}{2})[C_i U_i^1(\xi_i) + D_i U_i^2(\xi_i)], \tag{4}$$

where $\xi_i = \sqrt{\frac{m^*\omega_i}{\hbar}}(x - x_i^0)$, $\omega_i = \frac{eB_i}{m^*}$,

$$x_i^0(x) = \begin{cases} (m-1)(d_1+d_2) + \hbar k_y/eB_1, \\ (m-1)(d_1+d_2) \le x < md_1 + (m-1)d_2, \\ (m+1)d_1 + (m-1)d_2 - \hbar k_y/eB_1, \\ md_1 + (m-1)d_2 \le x < (m+1)d_1 + (m-1)d_2, \end{cases}$$

$$m = 1, 3, 5, \cdots, \tag{5a}$$

$$x_i^0(x) = \begin{cases} md_1 + (m-2)d_2 + \hbar k_y/eB_2, \\ md_1 + (m-2)d_2 \le x < md_1 + (m-1)d_2, \\ m(d_1+d_2) - \hbar k_y/eB_2, \\ md_1 + (m-1)d_2 \le x < m(d_1+d_2), \end{cases}$$

$$m = 2, 4, \cdots, \tag{5b}$$

C_i, D_i are arbitrary constants. U_i^1 and U_i^2 in equation (4) are Hermitian functions. Matching the wave function at the edges of magnetic barriers and wells, the transmission amplitude τ and the reflection amplitude r are obtained. Then, the transmission coefficient of electron transport through the finite MB superlattice is given by

$$T(E, k_y) = \frac{k_r}{k_l}|\tau|^2. \tag{6}$$

In the ballistic region, the conductance can be derived as the electron flow averaged over half the Fermi surface [15, 21]

$$G = G_0 \int_{-\pi/2}^{\pi/2} T(E_F, \sqrt{2E_F}\sin\phi)\cos\phi d\phi, \tag{7}$$

where ϕ is the angle of incidence relative to the x direction, E_F is the Fermi energy, $G_0 = e^2 m^* v_F l/\hbar^2$ with l the length of the structure in the y direction and v_F the Fermi velocity.

3 Results and discussions

In this section we discuss characteristics of transmission resonances in simple MB structures and features of resonance splitting in finite MB superlattices. Figure 2 presents the transmission coefficient versus incident energy for electrons tunneling through two DMBS's, two TMBS's and two QMBS's. Number n in each of the plots is the total number of building blocks in the corresponding structure. Structures considered here are arranged by block A ($B_1 = 0.1$ T and $d_1 = 1$) or by block A and block B ($B_2 = 0.3$ T and $d_2 = 1$) in AB sequence as depicted in Figure 1. In all six plots, solid, dashed and dotted curves are for $k_y = 0.0$, $k_y = 0.7$ and $k_y = -0.7$, respectively. Figure 2a1 shows results for the symmetric DMBS of two identical blocks A while Figure 2a2 is for the asymmetric DMBS which consists of two different blocks A and B. One can easily see that the transmission coefficient at resonances is always equal to unity for electrons tunneling through the symmetric structure whereas

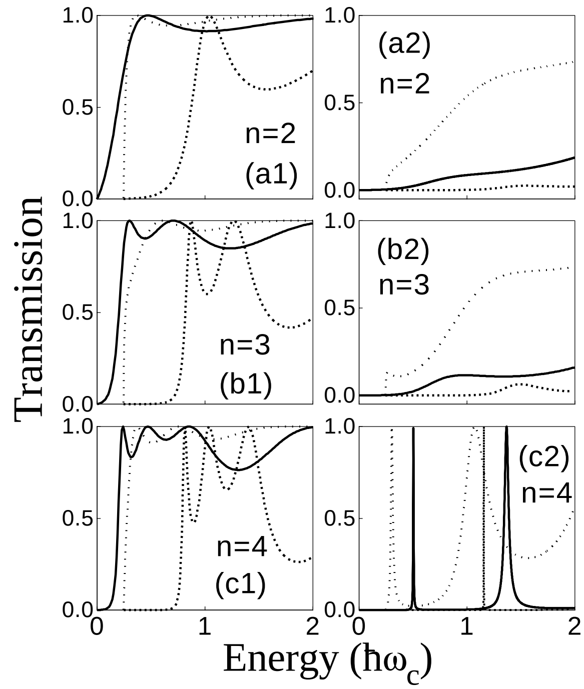

Fig. 2. Transmission through two DMBS's (see (a1) and (a2)), two TMBS's (see (b1) and (b2)), and two QMBS's (see (c1) and (c2)). In all plots, solid, dashed and dotted curves are for $k_y = 0, 0.7$ and -0.7, respectively. (a1), (b1) and (c1) are for structures of identical blocks A ($B_1 = 0.1$ T and $d_1 = 1$); (a2), (b2) and (c2) are for structures arranged by two different blocks A ($B_1 = 0.1$ T and $d_1 = 1$) and B ($B_2 = 0.3$ T and $d_2 = 1$).

transmission resonance peaks fall off rapidly in the asymmetric case. The larger the degree of the asymmetry of the structure, the smaller the transmission will become. These features reflect the fact that the asymmetric DMBS possesses stronger wave-vector filtering properties than the symmetric DMBS. Similar results have been obtained in reference [17] where there is a zero magnetic field region within barriers. The most obvious discrepancy in transmission resonances in this work from that in reference [17] is that we obtain fewer resonant peaks here. In this work, we carry out similar numerical calculations in order to see not only transition of transmission resonances but also in the following part to see resonance splitting effects in finite MB superlattices. The transmission for electron transport through two TMBS's are displayed in Figures 2b1 and 2b2. Two resonant peaks appear in Figure 2b1 for the TMBS of three identical blocks A for the $k_y \ge 0$ case. Only one suppressed peak can be seen in Figure 2b2 for the TMBS in which the middle block is twice the height as that of the right and the left ones. In this case one can see strong suppression of the transmission coefficient, as in the asymmetric DMBS. Figure 2c1 indicates the transmission spectrum for one QMBS of four identical blocks A, while Figure 2c2 is for another QMBS obtained by arranging two different blocks A and B. Three very sharp peaks can be seen in Figure 2c1 whereas the number of resonant peaks decreases and the width of peaks drastically narrows for the QMBS arranged with two different blocks. What strikes us most is that all peaks in the latter case cause no suppression and the transmission coefficient at resonances is always equal to unity. The results obtained here indicate that complete tunneling or 100% transmission can still occur in the QMBS of different building blocks. Comparing curves in Figure 2c2 with those in Figure 2a2 and in Figure 2b2, we can see that there exists a transition of transmission resonances for electrons tunneling through from simple MB structures to comparatively complex MB structures. In simple DMBS and TMBS (here both of them are arranged with two blocks with different heights and same widths), 100% transmission at resonances is not possible, while in complex MB structures arranged by the same two different blocks ($n \geq 4$), complete tunneling can occur as in MB structures of identical blocks.

Complete transmission resonances found in the QMBS obtained by arranging two different blocks seems to be connected with the superstructure of two identical larger blocks each consisting of two alternating building blocks. One may wonder what happens in a MB structure of an odd number of different building blocks. Are transmission resonances suppressed or not? In order to reveal the nature of transmission resonances in the MB structure of an odd number of different blocks, we show numerical results in Fig. 3 for three MB structures. The structures are obtained by periodically arranging two different blocks A ($B_1 = 0.1$ T and $d_1 = 1$) and B ($B_2 = 0.2$ T and $d_2 = 1$) in AB sequence. Here we lower the difference between two building blocks in order to see the transition which is introduced by the many barrier effect. For curves from top to bottom, corresponding total numbers of building blocks are of 5, 7 and 9, respectively. In all of our plots, solid, dashed and dot-dashed curves are for $k_y = 0.0$, $k_y = 0.7$ and $k_y = -0.7$, respectively. One can once again see 100% transmission resonances in all three cases. This feature indicates that complete transmission resonances in comparatively complex MB structure arranged by two different blocks is not closely connected with the superstructure of two identical larger blocks (each consisting of two alternating building blocks). We think it is driven by the many barrier effect.

There is another question one may wonder, *i.e.*, can complete transmission resonances appear in simple MB structures of unidentical blocks? In Figure 4 we display numerical results for one asymmetric DMBS (see Fig. 4a), one TMBS (see Fig. 4b) and one QMBS (see Fig. 4c). In this case, both the width and the height of two blocks are set to different values. $B_1 = 0.1$ T and $d_1 = 1.95$ are for block A, $B_2 = 0.3$ T and $d_2 = 1$ for block B. We carefully choose these parameters in order to get 100% transmission resonances for electrons with $k_y = 0.7$ tunneling through the DMBS. One can see that in simple DMBS and TMBS, complete tunneling indeed occurs at some k_y-value, while at other k_y-value, transmission resonances are suppressed as in the DMBS and TMBS where its building units are with different heights and same widths (see Figs. 2a2 and b2). To some extent features of transmission resonances exhibited in Figure 4 (such as, the total number of peaks

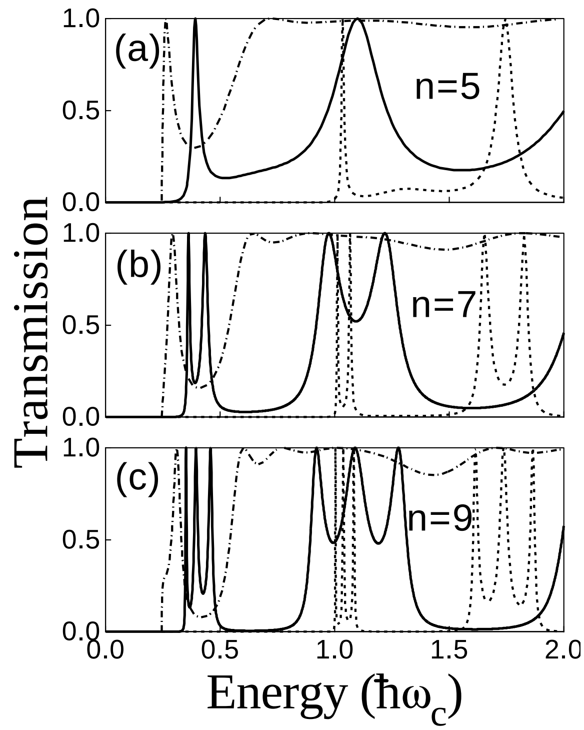

Fig. 3. Transmission through three complex MB structures which are periodically arranged by block A ($B_1 = 0.1$ T and $d_1 = 1$) and block B ($B_2 = 0.3$ T and $d_2 = 1$). The total numbers of building blocks are $n = 5, 7$ and 9 for the curves from top to the bottom. In all plots, solid, dashed and dot-dashed curves are for $k_y = 0, 0.7$ and -0.7, respectively.

and relative positions between them) are very similar to that for MB structures of identical blocks. This implies that high quality tunneling can also occur in MB structures of unidentical blocks. Another main feature which we should notice is that in similar DMBS's or TMBS's of unidentical blocks, it is impossible to obtain complete transmission resonances for any incident wave-vector k_y. That is to say, for different k_y, we should properly adjust parameters of building blocks in order to get optimum tunneling. From Figure 4c one can once again see a transition of transmission resonances for electrons tunneling through from simple MB structures to complex structures, especially for the $k_y = -0.7$ case. Moreover, in all three cases the width of peaks narrows drastically due to the increase of the width of the whole structure.

Most tunneling properties obtained in the MB structure [15,19] have been successfully explained by using the concept of the effective potential $V(E, k_y) = [A_i(x) + k_y]^2/2$ of MB structures. Here by using the same concept we can also explain the wave-vector-dependent transition (from incomplete transmission resonances to complete transmission resonances) in the simple MB structure, and the transition of transmission resonances for electrons tunneling through from simple MB structures to comparatively complex structures. First, we should notice the fact that the effective potential structure depends strongly not only on parameters of the MB structure but also on

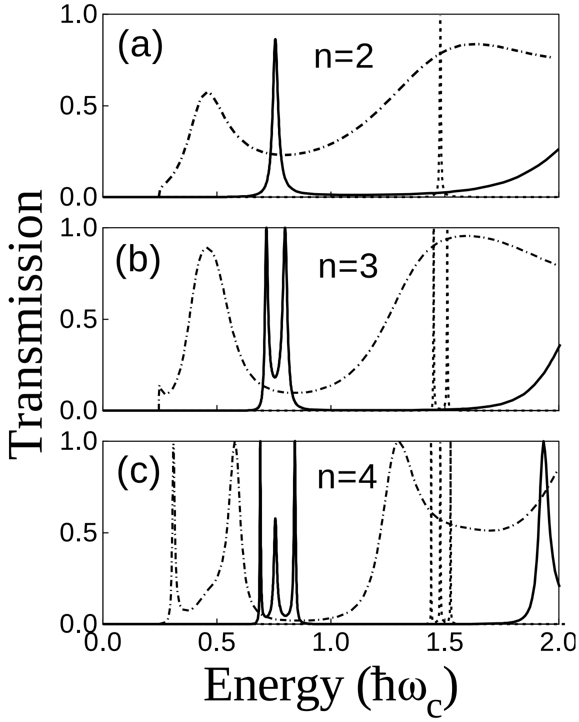

Fig. 4. Transmission through (a) one asymmetric DMBS ; (b) one TMBS; (c) one QMBS. The structures for (a), (b) and (c) are arranged by block A ($B_1 = 0.1$ T and $d_1 = 1.95$) and block B ($B_2 = 0.3$ T and $d_2 = 1$). In all plots, solid, dashed and dot-dashed curves are for $k_y = 0, 0.7$ and -0.7, respectively.

the wave-vector k_y. For the transport of electrons with $k_y > 0$ through a MB structure, the corresponding effective potential is electric barriers, and transport is the tunneling through barriers; whereas for the $k_y < 0$ case the corresponding effective potential is multiple-wells in which the process of electron motion is transport through a virtual state above quantum wells [15]. Secondly, we should notice another well-known fact, *i.e.*, the transmission coefficient at resonances is usually unity in a symmetric electric double-barrier structure. If an electric field is applied to the symmetric structure, the symmetric feature of the structure cannot be retained and the transmission coefficient at resonances is reduced. Because of the same reason, the resonant transmission coefficient in asymmetric double-barrier electric structure is small. However, complete tunneling can occur in asymmetric structures if the transmission coefficient for the left barrier is exactly the same as that for the right one [22]. In triple-barrier electric structures which consists of unidentical barriers, we can also obtain complete tunneling by properly adjusting parameters of the middle barrier and that of the side ones [23]. Therefore, keeping these facts in mind, we have no difficulty to understand the transition of transmission resonances found in the MB structure. For electron transport through MB structures of identical blocks, the potential profile of $V(E, k_y)$ is equivalent to electric barrier structures or well structures of identical blocks. So in this case we can see complete tunneling as in electric structures of identical barriers and wells. For electrons tunneling through MB structure of different blocks, the potential profile $V(E, k_y)$ is equivalent to electric structures of unidentical barriers or wells, and for different k_y the corresponding electric structure differ greatly. As an example, in an asymmetric DMBS consisting of block A ($B_1 = 0.1$ T and $d_1 = 1.95$) and block B ($B_2 = 0.3$ T and $d_2 = 1$), the transmission for the left block and right block at resonant energy is nearly the same for $k_y = 0.7$, whereas for other k_y-value this relation is broken. So we see complete transmission resonances for $k_y = 0.7$ case while for other k_y cases we only see incomplete transmission resonances. We can also explain the transition existing in the case where electrons tunnel through from simple MB structures to complex MB structures, from the point of view of the effective potential of MB structures and many barrier effect [23].

In Figures 5a to 5c we show the conductance for electron transport through three DMBS's, three TMBS's and three QMBS's. In all of our plots, solid, dotted and dot-dashed curves are for structures which are obtained by arranging one building block A ($B_1 = 0.1$ T and $d_1 = 1$), two different building blocks A ($B_1 = 0.1$ T and $d_1 = 1$) and B ($B_2 = 0.3$ T and $d_2 = 1$), and two blocks A ($B_1 = 0.1$ T and $d_1 = 1.95$) and B ($B_2 = 0.3$ T and $d_2 = 1$) in AB, ABA and ABAB sequences, respectively. It can be seen that there are shoulder structures of the conductance for two DMBS's which are of identical blocks, and of two blocks with different heights and same widths. However, for the DMBS of two blocks with different heights and different widths, one can see a sharp peak in low Fermi energy. The conductance is suppressed drastically for electron transport through two asymmetric DMBS's due to the averaging of the transmission $T(E, k_y)$ over half of the Fermi surface. Comparing Figure 5a with Figure 3a in reference [17], both quantitatively and qualitatively, there is significant difference in the conductance, especially for the symmetric DMBS. It is evident that the zero magnetic field region within magnetic barriers plays a very important role in electron transport through MB structures. From Figure 5b one can see a sharp peak and a shoulder structure in the dot-dashed curve for the TMBS which is arranged by two different blocks with very different heights and widths. A strong suppression effect of the conductance can be seen for two TMBS's of unidentical blocks due to the reduction of the transmission. In Figure 5c the conductance is presented for electron transport through three QMBS's. Besides a similar suppression effect of the conductance existing in two QMBS's arranged by two different blocks, we can also see that there are two sharp peaks (dotted curve) for the case arranged by two blocks with different heights and same widths, while in the other case we can see more peaks in which most of them are suppressed and only one peak has large peak-value. The features exhibited in the conductance reflect transitions of transmission resonances in MB structures of unidentical blocks.

For finite MB superlattices of more magnetic barriers and wells, we can also investigate tunneling transport

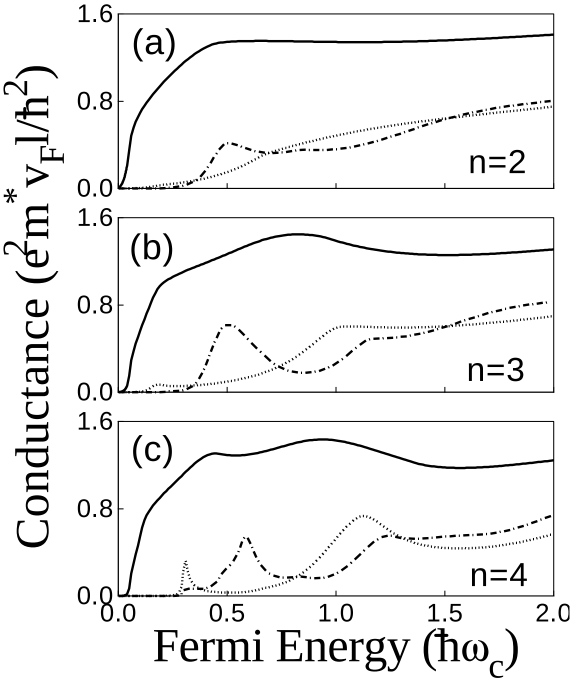

Fig. 5. Conductance through three DMBS's, three TMBS's and three QMBS's. In all plots, solids curves are for structures of identical blocks A ($B_1 = 0.1$ T and $d_1 = 1$); dotted curves are for structures arranged by two blocks A ($B_1 = 0.1$ T and $d_1 = 1$) and B ($B_2 = 0.3$ T and $d_2 = 1$); dot-dashed curves are for structures arranged by two blocks A ($B_1 = 0.1$ T and $d_1 = 1.95$) and B ($B_2 = 0.3$ T and $d_2 = 1$).

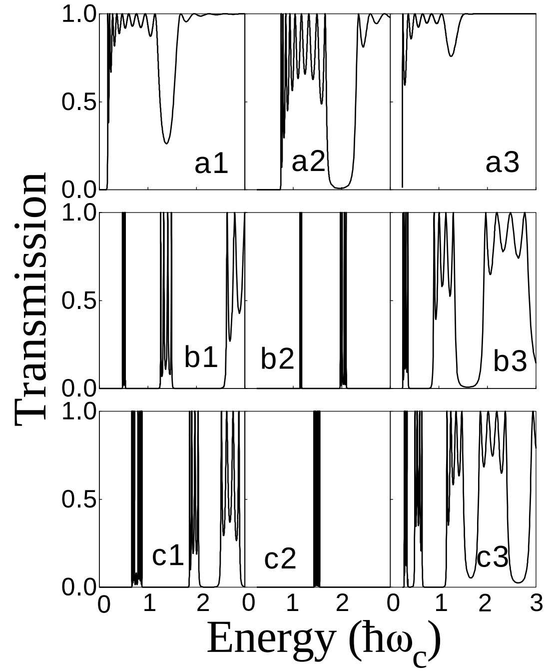

Fig. 6. Transmission spectrum through three finite MB superlattices of ten building blocks. (ai), (bi) and (ci) ($i = 1, 2, 3$) are for a superlattice of identical blocks A ($B_1 = 0.1$ T and $d_1 = 1$), a superlattice of periodically arranged two blocks A($B_1 = 0.1$ T and $d_1 = 1$) and B ($B_2 = 0.3$ T and $d_2 = 1$), and a superlattice of periodically arranged by block A ($B_1 = 0.1$ T and $d_1 = 1.95$) and block B ($B_2 = 0.3$ T and $d_2 = 1$), respectively. (a1), (b1) and (c1) : $k_y = 0.0$; (a2), (b2) and (c2): $k_y = 0.7$; (a3), (b3) and (c3) $k_y = -0.7$.

properties. Figure 6 presents numerical results of transmission coefficients *versus* incident energy for three finite MB superlattices which are obtained by periodically arranging one block A ($B_1 = 0.1$ T and $d_1 = 1$) (see (a1), (a2) and (a3)), two blocks A ($B_1 = 0.1$ T and $d_1 = 1$) and B ($B_2 = 0.3$ T and $d_2 = 1$) (see (b1), (b2) and (b3)), and two blocks A ($B_1 = 0.1$ T and $d_1 = 1.95$) and B ($B_2 = 0.3$ T and $d_2 = 1$) (see (c1), (c2), (c3)), respectively. The total number of building blocks in the three cases is set to be 10. Resonant and unresonant domains can be seen in the transmission spectrum for all three cases. The transmission spectrum is changed drastically in two cases of unidentical blocks. One resonant domain for the superlattice of identical blocks splits into two resonant domains for the superlattice by periodically arranging two different blocks with the same widths and different heights, and the total width of resonant domains drastically narrows and the total number of resonant peaks decreases for $k_y \geq 0$ cases. For different k_y, the variations of the width and positions of resonant domains are also different. These features reflect the wave-vector-dependent properties of transport in the MB structure. In the transmission spectrum for the MB superlattice periodically arranged by two blocks with different widths and different heights (see (c1), (c2) and (c3)), one can see there is one resonant domain which consists of ten resonant peaks for $k_y = 0.7$ case; more narrower domains can be seen for $k_y \leq 0$ cases. In each small resonant domain there is four peaks. The number of peaks is exactly the same as that in the other case of unidentical blocks. The main difference is that the width between two adjacent domain narrows in this case due to the larger width of the whole structure. We notice that the transmission coefficient at resonances is always equal to unity no matter whether the superlattice consists of identical blocks or unidentical blocks. Here we once again see the transition of transmission resonances from simple MB structure to complex MB superlattices. Figure 7 shows the conductance through three finite MB superlattices as a function of Fermi energy E_F. For two superlattices which are obtained by arranging two different blocks, the conductance decreases and curves shift rightwards in comparison to that of the superlattice of identical blocks. We can also see that in the former cases resonant spikes are resolved and become sharper, especially in the region of lower Fermi energy. These features indicate that properties of tunneling in the MB superlattice depend strongly on the geometry of the structure, especially on the parameters of adjacent magnetic barriers and wells.

Finally, we discuss the resonance splitting effect exhibited in electron transport through finite MB superlattices. As we introduced in Section 1, this effect in periodic electric superlattices at zero bias or at low bias ($V_{bias} \approx 0$) has been considered by a number of authors [3,4]. It is found that for n-barrier tunneling the splitting would be

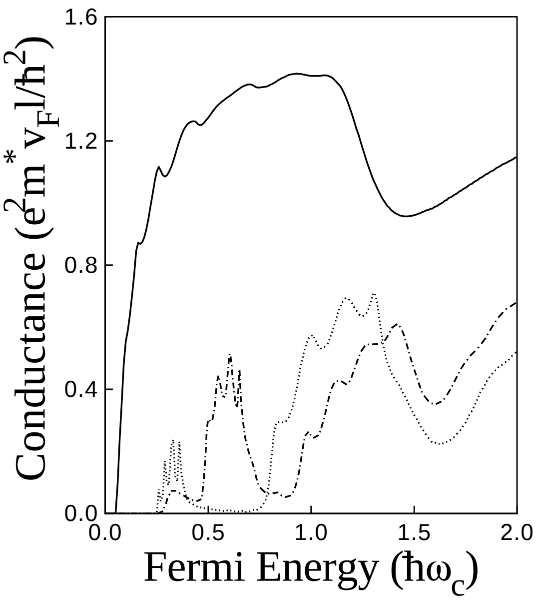

Fig. 7. Conductance through three finite MB superlattices. The parameters of three structures for solid, dotted and dot-dashed curves are exactly the same as that in Figure 6(ai), 6(bi) and 6(ci) ($i = 1, 2, 3$), respectively.

$(n-1)$-fold. In the MB superlattice the resonance splitting effect is more interesting and complex. We can hardly obtain a simple rule to generalize its main feature. It is evident from Figs. 2, 3, 4 and 6 that $(n-1)$-fold splitting for n-barrier tunneling can be extended to the MB structure periodically arranged by identical blocks through which electron with $k_y \geq 0$ transport, *i.e.*, for n-magnetic-barrier transport the splitting would be $(n-1)$-fold. The rule can not be extended to $k_y < 0$ case. One resonant domain in the MB superlattice arranged by identical blocks splits into two resonant domains in the MB superlattice which is periodically arranged by two blocks with different heights and the same widths. In the latter case, the splitting will occur each time two new blocks are added to the existing one. However, no matter what k_y-value electron possess, the total number of resonant peaks is no longer always equal to $(n-1)$. For the MB superlattice obtained by periodically arranging two different blocks with different widths and different heights, the splitting rule is also determined by parameters of building blocks and wave-vector k_y. However, its feature is more complex. In Figures 6c1, c2 and c3, for the $k_y > 0$ case, the splitting rule is similar to that for the $k_y \geq 0$ case in MB superlattices of identical blocks, whereas for the $k_y \leq 0$ case the splitting rule is similar to that in MB superlattices which are periodically arranged by two blocks with different heights and same widths. The resonance splitting effect can also be seen clearly in the conductance (see Fig. 7). We think that resonance splitting features exhibited in electron transport through finite MB superlattices is driven by magnetic miniband structures of corresponding MB superlattices. Because of the coupling between the effective wells *via* tunneling through effective barriers, the degenerate eigenlevels of the independent wells are split. Consequently, these levels redistribute themselves in groups around their unperturbed positions and form quasibands. Precisely speaking, for a finite MB superlattice, especially for a small n, there is no continuous energy band. In each magnetic miniband only some discrete and k_y-dependent energy could be expected. For a very large but finite n these levels form a quasi-continuous energy band. In comparison to the magnetic miniband of the MB superlattice of identical building blocks, minibands will split in the MB superlattice periodically arranged by two different blocks. In the latter case splitting features are determined not only by parameters of building blocks but also by wave vector k_y. Energy minibands in which allowed energy bands are separated by forbidden gaps. The total number of discrete energy levels and the width of the bands, and that of the gaps between them, depend on k_y. The necessary condition for the resonance in tunneling to occur is that the energy of the incident electron falls completely inside the allowed minibands. Therefore, in transmission spectrum and in the conductance for MB superlattices we can not only see resonant domains and unresonant domains but also see rich k_y-dependent and structure-induced resonance splitting phenomena.

4 Summary

In summary, we investigated transport properties, especially transitions of transmission resonances and resonance splitting effects in MB structures. It is confirmed that the transition of transmission resonances (between complete transmission and incomplete transmission) not only exists in the case for electron tunneling through from simple MB structures of identical blocks to simple structures of unidentical blocks but also exists in the case for electron transport through from simple MB structures of unidentical blocks to complex MB structures arranged by different blocks. In the simple unidentical block arranged structures, we can also obtain optimum transmission resonances by properly adjusting parameters of building blocks according to the k_y-value. However, it is impossible to get complete transmission resonances for any k_y-value in similar simple MB structures of two unidentical blocks. For electron tunneling through from simple MB structures to finite MB superlattices, the structure of the transmission spectrum changes significantly, *i.e.*, from solitary peaks to a cluster of peaks. Resonant domains in the transmission reflects the formation of magnetic minibands of energy, and the geometry of the structure largely affects the structure of the miniband. Through our studies on resonance splitting effect, we find that the rule obtained in the electric superlattice can not be extended to the MB superlattice directly. It is valid in the MB superlattice of identical magnetic barriers and wells through which electron with wave vector $k_y \geq 0$ tunnel. For a more complex superlattice with an arrangement of different blocks, splitting features are determined by both the parameters of building blocks and the wave-vector k_y of incident electron.

Two of us (Y. Guo and B.-L. Gu) would like to acknowledge partial support from the High Technology Research and Development Program of P.R. China.

References

1. L. Esaki, R. Tsu, IBM J. Res. Dev. **14**, 61 (1970).
2. L.L. Chang, L. Esaki, W.E. Howard, R. Ludeke, J. Vac. Sci. Technol. **10**, 11 (1973).
3. R. Tsu, L. Esaki, Appl. Phys. Lett. **22**, 562 (1973).
4. X.W. Liu, A.P. Stamp, Phys. Rev. B **50**, 1588 (1994).
5. M.A. McCord, D.D. Awschalom, Appl. Phys. Lett. **57**, 2153 (1990).
6. M.L. Leadbeater, S.J. Allen, J.F. DeRosa, J.P. Harbison, T. Sands, R. Ramesh, L.T. Florez, V.G. Keramidas, J. Appl. Phys. **69**, 4689 (1991); K.M. Krishnan, Appl. Phys. Lett. **61**, 2365 (1992); W.V. Roy, E.L. Carpi, M. Von Hove, A. Van Esch, R. Bogaerts, J. De Boeck, G. Borghs, J. Magn. Magn. Mater. **121**, 197 (1993); R. Yagi, Y. Iye, J. Phys. Soc. Jpn **62**, 1279 (1993).
7. A.K. Geim, Pis'ma Zh. Eksp. Teor. Fiz. **50**, 359 (1989) [JETP Lett. **50**, 389 (1990)]; S.J. Bending, K. von Klitzing, K. Ploog, Phys. Rev. Lett. **65**, 1060 (1990).
8. H.A. Carmona, A.K. Geim, A. Nogaret, P.C. Main, T.J. Foster, M. Henini, S.P. Beaumont, M.G. Blamire, Phys. Rev. Lett. **74**, 3009 (1995).
9. P.D. Ye, D. Weiss, R.R. Gerhardts, M. Seeger, K. von Klitzing, K. Eberl, H. Nickel, Phys. Rev. Lett. **74**, 3013 (1995).
10. S. Izawa, S. Katsumoto, A. Endo, Y. Iye, J. Phys. Soc. Jpn **64**, 706 (1995).
11. V. M. Ramaglia, A. Tagliacosso, F. Ventriglia, G.P. Zucchelli, Phys. Rev. B **43**, 2201 (1991); V.M. Ramaglia, F. Ventriglia, J. Phys. Condens. Matter **3**, 4881 (1991).
12. J.E. Müller, Phys. Rev. Lett. **68**, 385 (1992).
13. M. Calvo, Phys. Rev. B **48**, 2365 (1993); J. Phys. Condens. Matter **6**, 3329 (1994); Phys. Rev. B **51**, 2268 (1995).
14. C.L. Foden, M.L. Leadbeater, J.H. Burroughes, M. Pepper, J. Phys. Condens. Matter **6**, L127 (1994).
15. M. Matulis, F.M. Peeters, P. Vasilopoulos, Phys. Rev. Lett. **72**, 1518 (1994).
16. J.Q. You, L.D. Zhang, P.K. Ghosh, Phys. Rev. B **52**, 17243 (1995).
17. Y. Guo, B.L. Gu, W.H. Duan, Y. Zhang, Phys. Rev. B **55**, 9314 (1997).
18. J.Q. You, L.D. Zhang, Phys.Rev. B **54**, 1526 (1996).
19. I.S. Ibrahim, F.M. Peeters, Phys. Rev. B **52**, 17321 (1995).
20. Y. Guo, Y.C. Li, X.J. Kong, C.W. Wei, Phys. Rev. B **50**, 17249 (1994).
21. M. Büttiker, Phys. Rev. Lett. **59**, 1761 (1986).
22. X.D. Zhao, H. Yamamoto, K. Taniguchi, Appl. Phys. A **60**, 369 (1995).
23. X.D. Zhao, H. Yamamoto, Z.M. Chen, K. Taniguchi, J. Appl. Phys. **79**, 6966 (1996).